

Transfer learning of phase transitions in percolation and directed percolation

Jianmin Shen,¹ Feiyi Liu,^{1,2,*} Shiyang Chen,^{1,†} Dian Xu,¹ Xiangna Chen,¹ Shengfeng Deng,³ Wei Li,^{1,4} Gábor Papp,² and Chunbin Yang¹

¹*Key Laboratory of Quark and Lepton Physics (MOE) and Institute of Particle Physics, Central China Normal University, Wuhan 430079, China*

²*Institute for Physics, Eötvös Loránd University*

1/A Pázmány P. Sétány, H-1117, Budapest, Hungary

³*Institute of Technical Physics and Materials Science, Center for Energy Research, Budapest 1121, Hungary*

⁴*Max-Planck-Institute for Mathematics in the Sciences, 04103 Leipzig, Germany*

(Dated: January 7, 2022)

The latest advances of statistical physics have shown remarkable performance of machine learning in identifying phase transitions. In this paper, we apply domain adversarial neural network (DANN) based on transfer learning to studying non-equilibrium and equilibrium phase transition models, which are percolation model and directed percolation (DP) model, respectively. With the DANN, only a small fraction of input configurations (2d images) needs to be labeled, which is automatically chosen, in order to capture the critical point. To learn the DP model, the method is refined by an iterative procedure in determining the critical point, which is a prerequisite for the data collapse in calculating the critical exponent ν_{\perp} . We then apply the DANN to a two-dimensional site percolation with configurations filtered to include only the largest cluster which may contain the information related to the order parameter. The DANN learning of both models yields reliable results which are comparable to the ones from Monte Carlo simulations. Our study also shows that the DANN can achieve quite high accuracy at much lower cost, compared to the supervised learning.

I. INTRODUCTION

In the age of artificial intelligence, machine learning (ML) [1, 2] has promptly become a significant means of scientific research. Due to its great power in image recognition and feature extracting, a huge amount of complex data can be analysed handily in statistical physics [3–7], which provides us a new choice to deal with phase transitions beyond conventional field theory methods [8, 9] and Monte Carlo simulations [10].

Recently, the two major kinds of machine learning for phase transitions study are supervised [11–13] and unsupervised learning [14–19]. The difference between the two is that the former needs to label data while the latter does not, but the goals of both are to train models with better compatibility. In the field of phase transition, supervised learning mainly identifies or classifies phases of matter. Whereas unsupervised learning techniques, such as principal component analysis (PCA) [20, 21], stochastic neighbor embedding (T-SNE) [22, 23] and autoencoder [24–27] etc, are more suitable for clustering and dimensionality reduction. At present, a well

performed technique named transfer learning (TL) [28–32] mixing both labeled and unlabeled data, has been popular in dealing with images. It can not only obtain the critical exponent of the phase transition model through data collapse like supervised learning does, but extract the feature representation from the original data like unsupervised learning does. Additionally, TL has been used in community or module detection [33, 34], from where may also lead phase transitions. In reality data are rarely labeled since feature engineering with vast amount of data is time-consuming and computationally expensive. This fact thus gives rise to the emergence of TL, which has lately become a crucial branch of ML. The basic idea of TL is to enable the model to translate unlabeled data in target domain into labeled data in source domain. In Ref. [35] it has been proven that the domain adversarial neural network (DANN) has better performance than traditional neural networks (NN) and support vector machines (SVM) do. In Ref. [31], the DANN has also successfully identified paradigmatic phase transition models, including the Ising model, the Bose-Hubbard model, and the Su-Schrieffer-Heeger model with disorder, which opens the door for the study of many-body localization problem. We are therefore intrigued by the extent of effectiveness of DANN in traditional phase transition models, especially of non-equilibrium, which is the main motivation of this work.

* fyliu@mails.ccnucnu.edu.com

† shiyang-chen@mails.ccnucnu.edu.com

The adopted two models are directed percolation (DP) model and percolation model. These two models have broad applicability, as well as uniqueness of properties that have to be paid attention. The DP model [36, 37] represents the most important universality class of non-equilibrium phase transitions that we can understand so far [36–40], the DP universality class. Quite a few non-equilibrium models were confirmed to belong to the DP class. While the percolation model [41, 42] is a special one of equilibrium phase transition [8, 9], whose order parameter is not the particle density as in most models. In this paper we apply the DANN to the above two models, aiming at extracting essential information embedded at the critical regime. To improve the accuracy of measurements of critical points and critical exponents, a method to extend source domain is developed to expand our labeled set. Additionally, we examine when we expect the DANN to work properly.

The main structure of this paper is as follows. In Sec. II A, the two phase transitions models of interest will be given. Sec. II B gives the method of adversarial domain adaptation. Sec. II C includes the data sets and DANN learning results of the phase transitions models employed. In Sec. II D, we discuss our major findings. Sec. III is a summary of this work.

II. TRANSFER LEARNING OF PHASE TRANSITIONS

A. Models

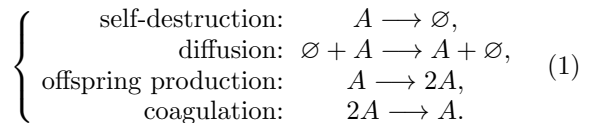
In the following we briefly introduce two models, a non-equilibrium directed bond percolation in 1+1 dimensions, and an equilibrium two-dimensional site percolation.

1. The DP model

Compared to equilibrium phase transitions, the non-equilibrium ones possess an extra time dimension. In this part, we focus on a class of phase transitions that involve absorbing states, where the time evolution stops [36, 37, 43, 44] and the system is stuck in inactive states. The physical nature of absorbing phase transitions is a competitive mechanism of proliferation and annihilation of quantities that can be particles, energy, molecules, viruses, and so on and so forth. Here, we first consider the DP model with only one absorbing state. The DP model represents one of the most significant class of

non-equilibrium phase transitions, the DP universality class. Lattice models like contact process (CP), Domany-Kinzel (DK) model, and pair-contact process (PCP), all belong to the DP universality class.

In the simplest version of bond DP, the evolution is done on a tilted (1+1) dimensional square lattice, and a bond is formed at the time step with probability p from an existing bond (see Fig. 1). Here, we are using periodic boundary conditions. This model may be interpreted as a reaction-diffusion process of interacting particles: representing the active particle as A and the empty site as \emptyset , the reaction-diffusion mechanism of DP is



ML techniques can process complex data produced by various lattice models of non-equilibrium phase transitions. These models include unitary or binary random reaction processes, which may contain diffusion or non-diffusion motions. Since within the universality class only the critical exponents are common and the position of the phase transition may vary, we fix the model to the above mentioned simplest case. Fig. 1 shows DP’s configurations generated from two different initial conditions, including a fully occupied lattice and a single active seed. In this paper we use the former one to generate configurations with different bond percolation probabilities.

For the (1+1)-dimensional bond DP, the order parameter can be expressed by the steady-state density [36],

$$\rho_a(p) \sim (p - p_c)^\beta, \quad (2)$$

where ρ_a denotes particle density and β represents a critical exponent. Since the density is encoded in the full configuration, we provide configurations exemplified in the left panel of Fig. 1 as an input to the DANN. Some care should be taken with the choice of the characteristic temporal length t_c , in order to achieve stable results. As shown in [36], due to scaling the proper choice of t_c is proportional to $L^{z/d}$, where $z = 1.580(1)$ and d is the spatial dimension of the percolation, and here $d = 1$.

2. The Percolation model

The second model for our study is the two-dimensional site percolation with periodic boundary

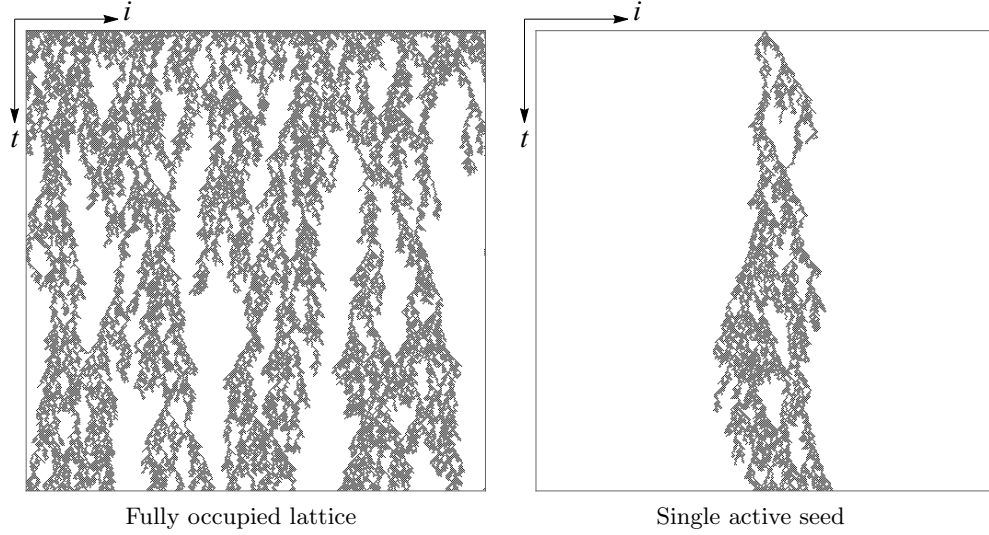


FIG. 1. The critical configurations of bond DP in (1+1) dimensions, starting from a fully occupied lattice (left panel) and from a single active seed (right panel), respectively, where $L = 500$, the time step is 500 and the bond probability p is 0.6447.

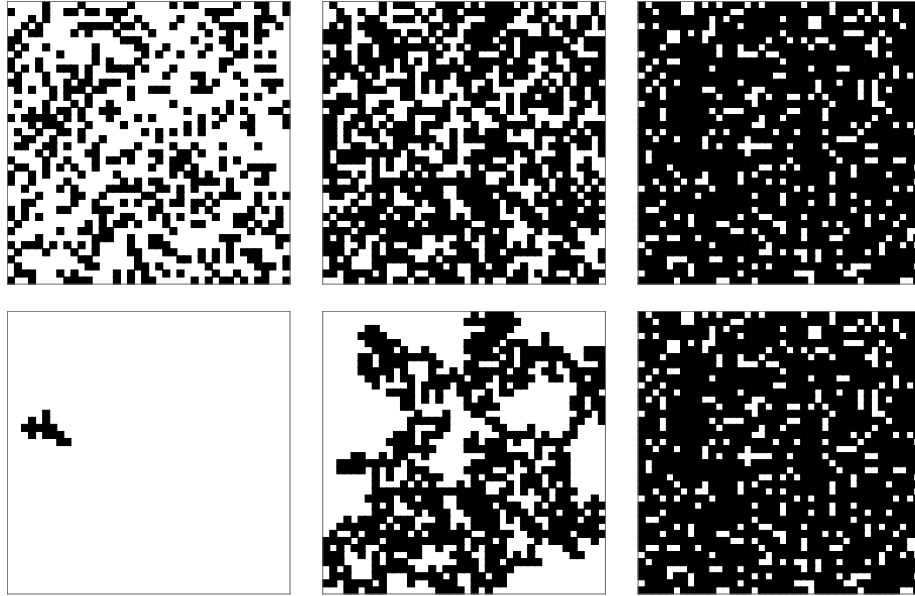


FIG. 2. The top panels are raw configurations of two-dimensional site percolation generated by probabilities 0.3, 0.593, and 0.8 respectively, where lattice size is 40. The bottom panels are corresponding, largest clusters generated from the top panels.

conditions, where the probability of a site being occupied is controlled by the probability p . A few typical configurations are shown in the upper panel of Fig. 2 at different occupation probabilities.

The order parameter of the site percolation is the

fraction of the sites $P_\infty(p)$ in the lattice belonging to the infinite cluster (for infinite lattice) or, for finite lattices belonging to the incipient infinite clusters or simply percolating clusters. An infinite system is percolating if only one cluster is infinite, while in fi-

nite systems the percolating cluster emerges as the occupied sites form a channel from top to down or left to right. The fraction $P_\infty(p)$ can be also identified with a probability of a site belonging to the percolating cluster, and around the critical point it scales with the critical exponent β [36] as,

$$P_\infty(p) \propto (p - p_c)^\beta \quad \text{for } p \rightarrow p_c^+. \quad (3)$$

Now, the order parameter is related to the largest cluster. Hence, using DANN for predicting the transition point, contrary to the DP case where the full configuration is provided as the input, here for percolation learning only the largest cluster is singled out as input. Namely, for each configuration only the sites belonging to the largest cluster are left, as shown in the lower panel of Fig. 2. For two-dimensional site percolation, the critical occupation value $p_c = 0.592746$ [42].

B. The domain adversarial neural network(DANN) method

To find out the parameters of the phase transitions, we construct a DANN, feeding it with the configurations as in Fig. 1 for (1+1)- dimensional directed bond percolation and as in the lower part of Fig. 2 for two-dimensional site percolation. The architecture of the network is the same for the two models which are trained, however, separately.

The major obstacle for applying the neural networks, most of which are density based training methods, to phase transitions for physics models is the lacking of labeled data near critical points, which may cause the supervised network prediction of critical points to deviate from the genuine results [45]. We choose here DANN, because it is expected to predict the critical points more accurately compared to the traditional perception network [35]. A performance comparison between the traditional NN and DANN will be given in Sec. IID2. The detailed mechanism of DANN approach is written as follows.

The prepared training dataset is divided into two parts: a source domain and a target domain. The source domain consists of labeled data x with data density distribution $P(x)$, and the target domain contains all the unlabeled data χ only with distribution $P(\chi)$. DANN predicts the label of the configuration χ through finding its similarities with the labeled dataset $\{x\}$. The basic components of DANN are feature extractor, label predictor and domain classifier, as shown in Fig. 3. The feature extractor (green), is used to generate the latent variable

(feature vector) for labeled data or unlabeled data from those two domains, and those feature variables are fed into the label predictor and domain classifier. Using the feature vector, the label predictor (blue) predicts the corresponding label for labeled data and also for the unlabeled one after training. The output of label predictor is a two- dimensional vector: the probabilities of the configurations belonging to category “0” (nonpercolating phase, i.e., $p < p_c$) and category “1” (percolating phase, i.e., $p > p_c$), respectively. Due to the softmax activator, the sum of elements of the vector is always 1.

On the other side, the domain classifier (red) determines the domain of the input from the feature vector: it is either ‘source’ (labeled) or ‘target’ (unlabeled). Our goal is to extract domain independent features, i.e., maximize the accuracy of the label predictor without being able to separate the domains. Hence, to optimize the network, the loss functions of the feature extractor, label predictor and domain classifier are formulated as

$$L_{lp} = L_y, \quad (4)$$

$$L_{fe} = L_y - L_d, \quad (5)$$

$$L_{dc} = L_d, \quad (6)$$

where L_y stands for the softmax cross entropy loss term for labeled data set, and L_d is the domain loss as

$$L_d = E_{P(x)}[\log(1 - P(x))] + E_{P(\chi)}[\log(P(\chi))]. \quad (7)$$

Note, that the domain classification loss (7) appears with opposite signs in the gradient descent for the feature extractor and the domain classifier. This trick forces DANN to do its best to classify domains and in parallel, to find features in the feature extractor, which contain the minimum possible information about domains.

This optimization has an adversarial character and leads the feature extractor to produce a domain invariant feature vectors so that the domain classifier can’t distinguish the data source. Consequently, it is also expected to reduce the effects from the different possible uneven sampling of the configurations [45]. After training the network predicts for the unlabeled data the probabilities to belong to classes “0” and “1”, respectively. For a specific theoretical explanation of this network structure, please refer to [45].

The structure of the DANN is indicated in Fig. 3 and the feature extractor part specifically, is shown in Fig. 4. It is based on a convolutional neural network (CNN) and a fully connected network (FCN) layer.

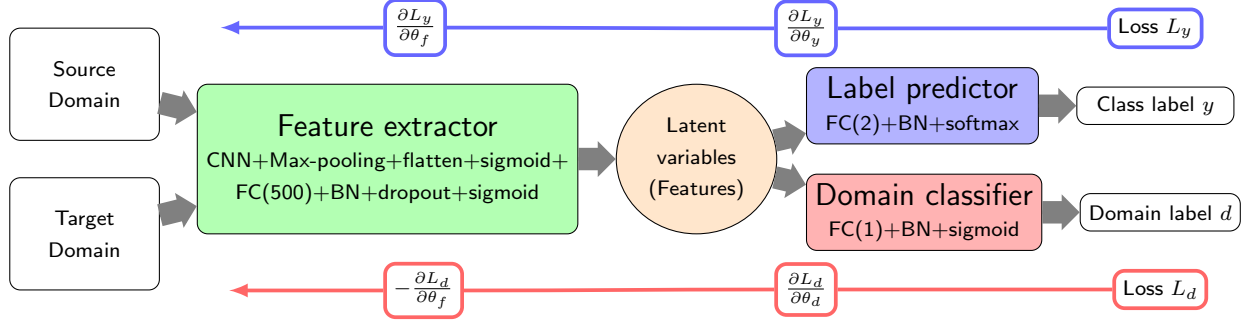


FIG. 3. The neural network schematic structure of adversarial domain adaptation. $\theta_f, \theta_d, \theta_y$ are the parameters for the feature extractor, domain classifier and label predictor, respectively. In the training of the feature extractor (green) the normal feedback propagation is inverted for the classifier parameters in order to create classification independent features. The ‘Feature extractor’ is shown in Fig. 4.

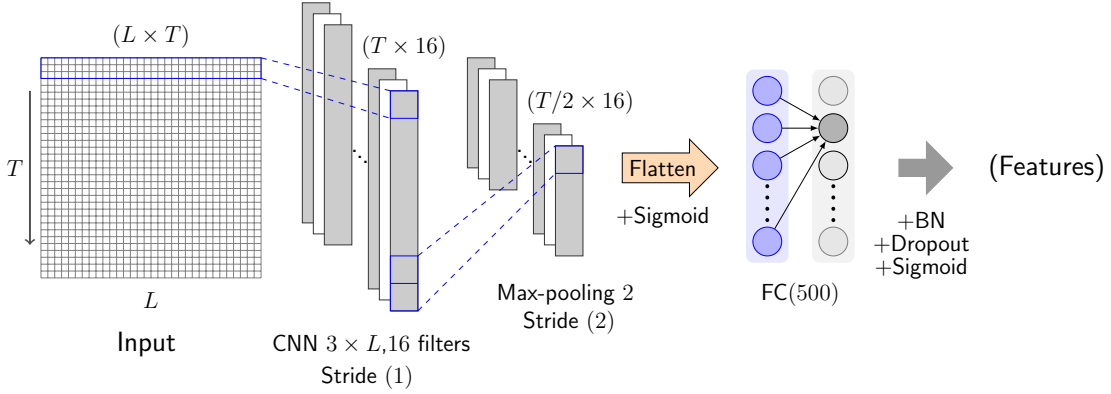


FIG. 4. The structure of feature extractor for the input of a two-dimensional system of size $L \times T$.

The input of the network is $L \times T$ images as given in Fig. 1 (bond DP model, $T = L^z$) or in the lower part of Fig. 2 (2-dimensional site percolation, $T = L$). The images are convoluted by a kernel of size $3 \times L$ into 16 filters, and the results are reduced by a factor of 2 by the max-pooling layer. Next, we apply a flattening layer resulting a vector of size $T/2 \times 16$, followed by a sigmoid activation. Finally, we apply a fully connected layer with 500 neurons. The feature vectors are produced by applying additional batch normalization, dropout (with rate 0.8) and hard sigmoid map. The label predictor and domain classifier have a very similar architecture based on a fully connected layer, except the difference in dimension and the activation function. In the label predictor we have 2 neurons and the softmax activation function, while the domain classifier has only 1 neuron with hard sigmoid activation function. We also apply batch normalization for both before data flow passes through the activation function. The

Adam optimizer [46] is used to speed up the training process of our neural network. Our adversarial domain adaptation is implemented based on TensorFlow 1.15 on AMD VEGA56 GPU platform.

C. The DANN results

1. Data sets of models

In order to implement the program sketch above, one needs to prepare the datasets: the full configurations for the DP and the largest cluster configurations for the site percolation. Furthermore, we need to label part of the data. Since our goal is to minimize the human intervention, we automatically label each configuration far away from the critical regime of the phase transition as “0” below the phase transition (configuration dies out for DP, or, percolating

cluster is missing for site percolation), and as “1” above the phase transition. Since for systems large enough, the transition is usually quite sharp, keeping “appropriate distance” from the transition point, and the number of mislabeled configurations is negligible, and should be handled properly by the network through the classification. In the paper we use the criterion for the “appropriate distance” that for given probability p all the configurations have in 99% the same DANN predicted label. Hence, for both models studied, we chose configurations generated in the p range $[0, 0.1] \cup [0.9, 1]$ to be the initial source domain with all configurations in the range $[0, 0.1]$ having label “0” and those in the $[0.9, 1]$ having label “1”. All the other configurations are considered to be in the target domain and unlabeled. Since in this paper we sampled the parameter p at 41 values chosen from the range $[0, 1]$ uniformly, and for each value we have generated 2000 samples, the number of configurations in the target domain is much larger than the ones in the source domain. For teaching we used 1000 epochs for each training set.

After training, we use the target domain configurations to predict the classification of a configuration at each value of p and average them for each p , separately. The transition point of p is found, when half of the configurations belongs to class “0” and the other half to “1”. To obtain the critical point of a model for an infinite system, we calculate the critical points at different system sizes ($L = 16, 32, 48, 64, 80$), and extrapolate the results to an infinite system using linear regression in $1/L$.

2. Finding the optimal source domain

Since the chosen source domain is quite far from the expected transition point, in the following we are trying to narrow down the region of the transition, extending the original $[0, 0.1] \cup [0.9, 1]$ support, iteratively. We start from $[0, l] \cup [r, 1]$ support with $l = 0.1$ and $r = 0.9$, estimating the transition probability p_c^0 with DANN, and update the domain parameters as

$$l^{(i+1)} = \frac{l^{(i)} + p_c^{(i)}}{2}, \quad r^{(i+1)} = \frac{r^{(i)} + p_c^{(i)}}{2}. \quad (8)$$

Next, we check whether the new bounds ($l^{(i+1)}$ and $r^{(i+1)}$) fulfill the condition, based on which the datasets are categorized with at least 99% confidence into any of the two phases. If not, the value of the bound is shifted closer to the original value, for instance $l^{(i+1),1} \rightarrow (l^{(i+1),0})/2$, and the correction is done while the confidence condition is not satisfied.

The procedure is stopped, when the support can not be longer extended on the dataset. The procedure is demonstrated in Fig. 5b.

3. Bond DP

After training the DANN on the optimal source domain for (1+1)-dimensional bond DP at $L = 32$, we evaluate the samples at different bond probabilities p , letting DANN to categorize them as either phase “0” or phase “1”. On the output side, DANN returns a probability for each configuration’s belonging to phase “0”. The average values of the probabilities belonging to phase “0” ($prob_0$) are shown in Fig. 5a, with a sigmoid fit. At the critical bond probability p_c , the probabilities of phases “0” and “1” are equal with each being $1/2$.

Fig. 5b illustrates the evolution of the optimal source domain support. The final target domain support is indicated by a grey region in Fig. 5a. Note, that already using the very limited starting source domain ($[0, 0.1] \cup [0.9, 1]$) for DANN results in a reasonable estimation for the transition point.

In order to get the critical bond probability for the infinite system, we have trained the DANN at different sizes, and extrapolated the results to zero on the $1/L$ scale, as shown in Fig. 6a. The obtained critical value of (1+1)-dimensional bond DP $p_c = 0.6453 \pm 0.0005$ is in agreement with the ‘standard’ value of 0.6447 [36].

Using the technique of data collapse, we may obtain the value of ν_\perp , the critical exponent of the spatial correlation length. The scaling $(p - p_c)L^{1/\nu_\perp}$ is universal [36], and from our results at lattice sizes of $L = 16, 32, 48, 64$ and 80 we may identify a proper ν_\perp to obtain the scaling (see Figs. 6b-c). Our value $\nu_\perp \simeq 1.09 \pm 0.06$ is in agreement within 1σ with the ‘standard’ value of 1.09 [36]. We should notice that the critical exponent is not a direct result of the DANN learning, but its determination relies on the critical bond probability p_c predicted by the DANN. Therefore, the accuracy of ν_\perp is related to that of p_c .

4. Site Percolation

In the previous section, we have applied DANN to a non-equilibrium phase transition model, and found that it can find the transition point in a many-body localization problem. To check the versatility of DANN, we intend to apply it to a specific equilib-

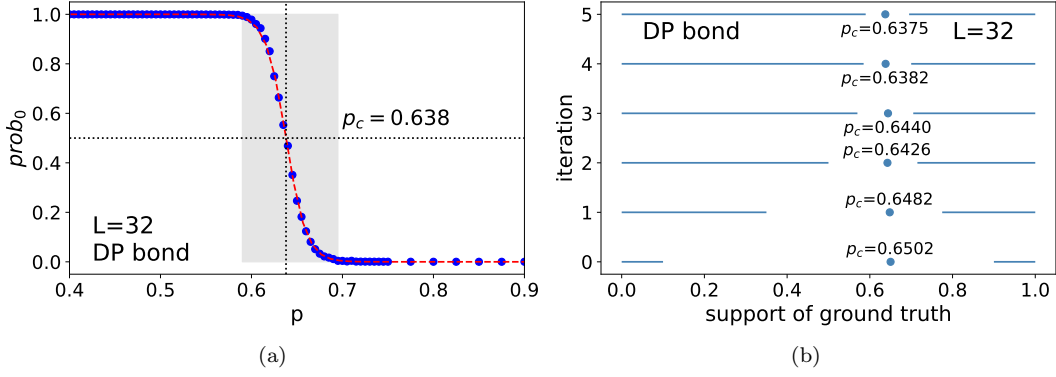


FIG. 5. **(a)** Average probability of belonging to phase “0” ($prob_0$) for DP bond percolation at $L = 32$, as a function of the bond probability p . The shadowed region indicates the target domain at the optimal support, and the dashed red line is the sigmoid fitting to the data. Its position parameter defines the critical probability p_c . **(b)** Evolution of the optimal domain support, and the corresponding critical bond probability values.

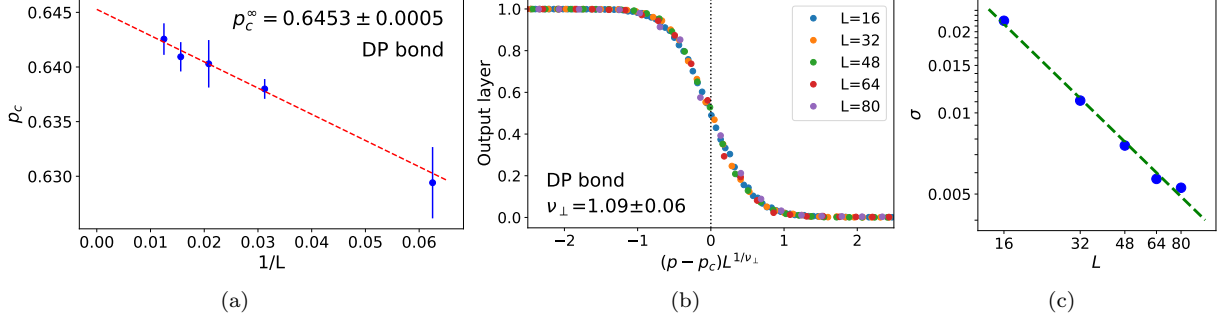


FIG. 6. **(a)** Extrapolation of the critical probability p_c to infinite lattice size for (1+1) bond DP. **(b)** ‘Data collapse’ rescaling of the results for different sizes. **(c)** Fit of the critical exponent ν_\perp using the width of the sigmoid fits.

rium phase transition, the two-dimensional site percolation. In site percolation, each site is occupied by a probability p , hence the particle density depends proportionally on this probability, and is therefore not an order parameter. Hence, the full configuration, carrying information primarily on the density, can not directly reveal the order parameter.

The order parameter for site percolation is the probability of a site belonging to the infinite (percolating) cluster. For finite systems it can be related to the size of the largest cluster. So here we will only analyze the largest cluster: from a full configuration (upper part of Fig. 2) we leave out all the sites not belonging to the largest cluster (lower part of Fig. 2). To illustrate the strong dependence of ML algorithms on the choice of data we present the learning result in Sec. IID 1, as a comparison, where DANN is trained with the full configurations.

We use the same DANN architecture as in the pre-

vious section and start again presenting result obtained on a $L = 32$ lattice in Fig. 7. The sigmoid fit with the target domain window is presented on the left, and the determination of the optimal source domain support, on the right. Again, the procedure is repeated for sizes $L = 16, 32, 48, 64$ and 80 , and the critical site occupation probability is extrapolated to the infinite system in Fig. 8. The DANN result $p_c = 0.5926 \pm 0.002$ is consistent with the numerical result 0.5927 [42], within 1σ . The correlation exponent is obtained similarly to the DP case using data collapse, yielding $\nu \simeq 1.29 \pm 0.03$, close to $\nu = 4/3$ from [42].

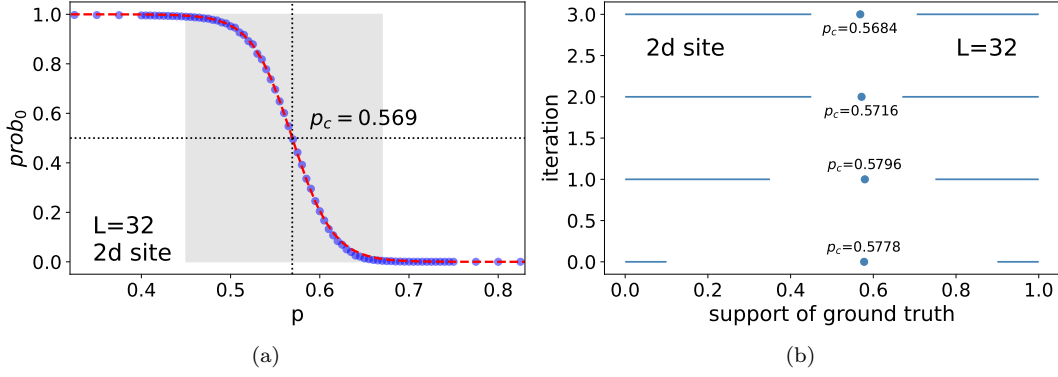


FIG. 7. **(a)** Average probability of belonging to phase “0” ($probo$) for two-dimensional site percolation at $L = 32$, as a function of the occupation probability p . The shadowed region indicates the target domain at the optimal support, and the dashed red line is the sigmoid fitted to the data. Its position parameter defines the critical probability p_c . **(b)** Evolution of the optimal domain support, and the corresponding critical bond probability values.

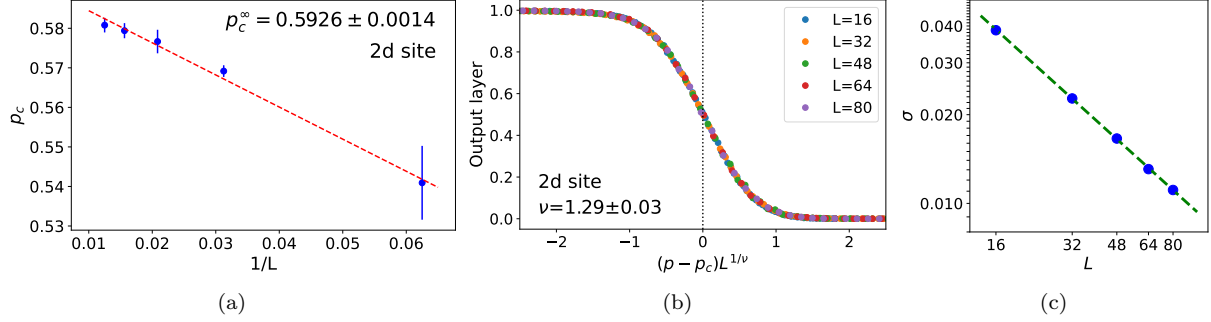


FIG. 8. **(a)** Extrapolation of the critical probability p_c to infinite lattice size for two-dimensional site percolation. **(b)** ‘Data collapse’ rescaling of the results for different sizes. **(c)** Fit of the critical exponent ν using the width of the sigmoid fits.

D. Discussions

1. Data preprocessing for DANN analysis

So far we have shown that DANN performs well in identifying phase transitions of the bond DP and site percolation in section II C. However, there is extra cost in a good representation of input data that can unveil the order parameters in a direct or an indirect way. In bond DP model, the order parameter is the occupation density that directly links to raw configurations. The features, or the occupation density here, of marginal data density are accessible so that the performance of DANN is outstanding. Similar observations were made in connection to the Ising model [47, 48], where the order parameter, the magnetization $M = \sum_i s_i/N$, has to be included to

the loss function (together with the energy) to reproduce the known results with good accuracy. Applying the principle component analysis in [14], the magnetization was identified as the order parameter, implying that the method may work for more complicated systems. For site percolation Ref. [13] developed a FCN and a CNN based model to detect the phase transition. Encouraged by this, using a more elaborated DL model we hope to develop in the future a network model capable of extracting the phase transition point using only raw configurations.

To illustrate the limitations of the present method(DANN), let us now try to use the raw configurations for the two-dimensional site percolation problem, instead of the largest cluster configurations. While the latter carries information about the order parameter directly, for the former it is not the case. Repeating the technique described

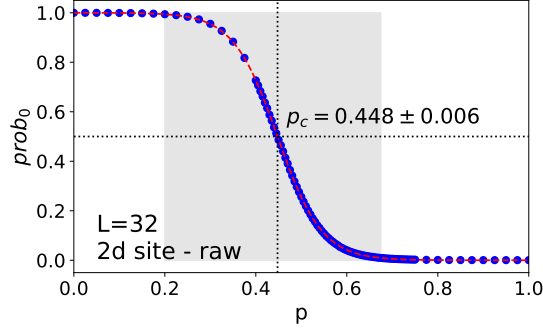


FIG. 9. DANN results of two-dimensional site percolation with *raw* configuration as input to DANN at $L = 32$. The shadowed region is the target domain at its optimal value, and is much broader than the one for the largest cluster configurations. The learned critical probability is much lower than the genuine one.

	exponents	Literature [36, 42]	Supervised Learning [13, 15]	DANN
Directed percolation	p_c	0.6447	0.6408	0.6453(5)
	ν_\perp	1.09	1.09(2)	1.09(6)
Site percolation	p_c	0.5927	0.594(2)	0.5926(2)
	ν	4/3	4/3	1.29(3)

TABLE I. DANN learning results of (1+1)-dimensional bond DP and two-dimensional site percolation.

in section IIC for the optimal source domain we gain a falsely predicted critical occupation probability $p_c \simeq 0.436$ at $L = 32$ (see Fig. 9), which is much smaller than the one obtained from using the largest cluster configurations, or equivalently the genuine critical point. From another point of view, the DANN, and many other ML algorithms as well, have the power of identifying the transition point, if applicable, embedded in the configurations. But the transition point may not be the actual critical point governed by the order parameter. Further information regarding the order parameter has to be compiled, which is then transferred to the learning algorithm.

2. Comparison of the DANN results with supervised learning

The models of interest (the directed (1+1) dimensional bond percolation and the two-dimensional site percolation of square lattice) have already been extensively investigated by different theoretical models (like e.g. mean-field, renormalization group), numerical Monte-Carlo simulations [36, 42], or, supervised learning [13, 15]. We compared major previous studies with the present study in Table I.

From the comparison we conclude that for this two models DANN performs nearly as well as the super-

vised learning does. Clearly the latter requires extra work as one has to label the different configurations.

To check the power of DANN in exploiting unknown regions, we perform the following test: we build a network similar to the DANN, leaving out the classification part (that is, dropping the adversarial character), and train the resulting networks on the optimal support of the source domain, calculated for the DANN. On the left support (source domain $[0, 0.1] \cap [0.9, 1]$) we mark each configuration as belonging to phase “0”, on the right to phase “1”. The results for $L = 32$ are presented in Fig. 10, where the shadowed region indicates the target domain (i.e. the domain without labels which are not presented to the non-adversarial network during training), showing a small, but noticeable shift in the transition point from the DANN values: 0.633 instead of 0.638 for DP, and 0.565 instead of 0.568 for two-dimensional site percolation. The difference is much more pronounced for the starting support of the source domain, $[0, 0.1] \cup [0.9, 1]$ (0.6152 instead of 0.6502 for DP, and 0.5975 instead of 0.5778 for two-dimensional site percolation), indicating that despite using a very limited dataset, the DANN is able to produce more reliable result than a non-adversarial network is.

The study shows DANN’s high perception ability for a limited training set. Naturally, when reliable labeling can be done (without too much effort) for

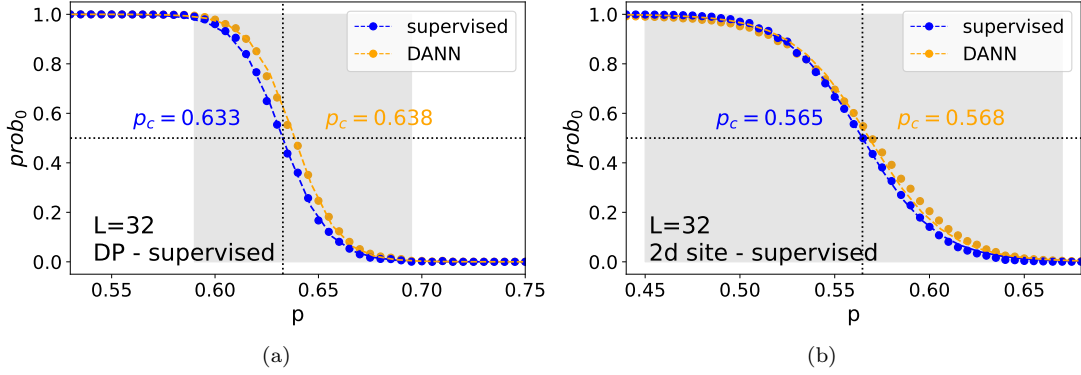


FIG. 10. Supervised learning versus DANN learning of (a) (1+1) bond DP and (b) two-dimensional site percolation models at size $L = 32$.

large dataset even close to the transition point, supervised learning should produce a more accurate result.

III. CONCLUSION

In this paper, we have applied a semi-supervised or transfer learning approach, the domain adversarial neural network (DANN), to detecting the critical points of phase transitions. Specifically, to explore the applicability of the DANN method, we have studied two kinds of models, the (1+1)-dimensional bond directed percolation as a representative of non-equilibrium systems and the two-dimensional site percolation as one of equilibrium systems. For (1+1)-dimensional bond DP model, we demonstrate how one may find the critical point p_c and calculate the critical exponent ν_\perp . Introducing an iterative approach to extend the source domain of the DANN, we are able to reproduce with high precision the genuine results for the transition point and critical exponent, using much smaller set of configurations than the Monte-Carlo methods.

In two-dimensional site percolation, we have shown that a careful preprocessing of the input data related to the order parameter should be applied to speeding up the training and improving the accuracy. Specifically, the largest cluster is singled out from the full configuration as input. Our conclusion is that DANN is a powerful method in determining the location of the critical point, and the spatial correlation exponent as well, with good accuracy and minimal computational cost. The method is then combined to the data collapse techniques, in order to have finite-size effects and then yield the values

corresponding to the infinite system.

We also noted that in the present form the DANN is very sensitive to the input configuration, as it expects configurations directly related to the order parameter. Presenting the network with raw configurations of two-dimensional site percolation the accuracy of the result is dropped tremendously. This issue will be systematically studied in the near future, by enabling the network to acquire automatically the relevant parts of the configuration, hopefully also in systems where the order parameter is more explicit.

The biggest advantage of DANN is its predictive power. Supervised learning assumes that the phase transition point is already known, and then predicts the accurate location by learning the information of this known range. DANN is able to predict quite accurately the location of the transition point already from very limited labelled information: a non-adversarial network using the same information can only obtain a much less precise result. On the other hand, a non-adversarial network learns more easily the relevant part of the configuration ('pre-filtering'), since it is presented with much more labelled data.

IV. ACKNOWLEDGEMENTS

We would like to thank Zhencheng Fu and Hongwei Tan for their helpful suggestions at the beginning of this work. This work was supported in part by the Fundamental Research Funds for the Central Universities, China (Grant No. CCNU19QN029), the National Natural Science Foundation of China (Grant No. 11505071, 61702207 and 61873104), the 111 Project, with Grant No. BP0820038, the

-
- [1] M. I. Jordan and T. M. Mitchell, *Science* **349**, 255 (2015).
 - [2] I. Goodfellow, Y. Bengio, and A. Courville, *Deep learning* **1**, 98 (2016).
 - [3] A. Engel and C. Van den Broeck, *Statistical mechanics of learning* (Cambridge University Press, 2001).
 - [4] P. Mehta and D. J. Schwab, *arXiv preprint arXiv:1410.3831* (2014).
 - [5] P. Mehta, M. Bukov, C.-H. Wang, A. G. Day, C. Richardson, C. K. Fisher, and D. J. Schwab, *Physics reports* **810**, 1 (2019).
 - [6] G. Carleo, I. Cirac, K. Cranmer, L. Daudet, M. Schuld, N. Tishby, L. Vogt-Maranto, and L. Zdeborová, *Reviews of Modern Physics* **91**, 045002 (2019).
 - [7] J. Carrasquilla, *Advances in Physics: X* **5**, 1797528 (2020).
 - [8] C. Domb, *The critical point: a historical introduction to the modern theory of critical phenomena* (CRC Press, 1996).
 - [9] D. J. Amit and V. Martin-Mayor, *Field Theory, the Renormalization Group, and Critical Phenomena: Graphs to Computers Third Edition* (World Scientific Publishing Company, 2005).
 - [10] J. Hammersley, *Monte carlo methods* (Springer Science & Business Media, 2013).
 - [11] J. Carrasquilla and R. G. Melko, *Nature Physics* **13**, 431 (2017).
 - [12] E. P. Van Nieuwenburg, Y.-H. Liu, and S. D. Huber, *Nature Physics* **13**, 435 (2017).
 - [13] W. Zhang, J. Liu, and T.-C. Wei, *Physical Review E* **99**, 032142 (2019).
 - [14] L. Wang, *Physical Review B* **94**, 195105 (2016).
 - [15] J. Shen, W. Li, S. Deng, and T. Zhang, *Physical Review E* **103**, 052140 (2021).
 - [16] S. J. Wetzel, *Physical Review E* **96**, 022140 (2017).
 - [17] W. Hu, R. R. Singh, and R. T. Scalettar, *Physical Review E* **95**, 062122 (2017).
 - [18] C. Wang and H. Zhai, *Physical Review B* **96**, 144432 (2017).
 - [19] J. Wang, W. Zhang, T. Hua, and T.-C. Wei, *Physical Review Research* **3**, 013074 (2021).
 - [20] K. Pearson, *The London, Edinburgh, and Dublin Philosophical Magazine and Journal of Science* **2**, 559 (1901).
 - [21] H. Abdi and L. J. Williams, *Wiley interdisciplinary reviews: computational statistics* **2**, 433 (2010).
 - [22] L. Van der Maaten and G. Hinton, *Journal of machine learning research* **9** (2008).
 - [23] L. Van Der Maaten, *The Journal of Machine Learning Research* **15**, 3221 (2014).
 - [24] H. Bourlard and Y. Kamp, *Biological cybernetics* **59**, 291 (1988).
 - [25] G. E. Hinton and R. S. Zemel, *Advances in neural information processing systems* **6**, 3 (1994).
 - [26] G. E. Hinton and R. R. Salakhutdinov, *science* **313**, 504 (2006).
 - [27] J. Shen, W. Li, S. Deng, D. Xu, S. Chen, and F. Liu, *Machine learning of pair-contact process with diffusion* (2021), *arXiv:2112.00489 [cond-mat.stat-mech]*.
 - [28] W. M. Kouw and M. Loog, *arXiv preprint arXiv:1812.11806* (2018).
 - [29] W. Xu, J. He, and Y. Shu, *Advances and Applications in Deep Learning* , 45 (2020).
 - [30] K. Ch'Ng, J. Carrasquilla, R. G. Melko, and E. Khatami, *Physical Review X* **7**, 031038 (2017).
 - [31] P. Huembeli, A. Dauphin, and P. Wittek, *Physical Review B* **97**, 134109 (2018).
 - [32] L. Malo Roset, *Applications of machine learning to studies of quantum phase transitions*, Master's thesis, Universitat Politècnica de Catalunya (2019).
 - [33] E. Eaton and R. Mansbach, in *Proceedings of the AAAI Conference on Artificial Intelligence*, Vol. 26 (2012).
 - [34] P. Zhang, C. Moore, and L. Zdeborová, *Physical Review E* **90**, 052802 (2014).
 - [35] H. Ajakan, P. Germain, H. Larochelle, F. Laviolette, and M. Marchand, *arXiv preprint arXiv:1412.4446* (2014).
 - [36] H. Hinrichsen, *Advances in physics* **49**, 815 (2000).
 - [37] S. Lübeck, *International Journal of Modern Physics B* **18**, 3977 (2004).
 - [38] G. Ódor, *Reviews of Modern Physics* **76**, 663–724 (2004).
 - [39] M. Henkel, H. Hinrichsen, S. Lübeck, and M. Pleimling, *Non-equilibrium phase transitions*, Vol. 1 (Springer, 2008).
 - [40] H. Haken, *Reviews of Modern Physics* **47**, 67 (1975).
 - [41] J. W. Essam, *Reports on progress in physics* **43**, 833 (1980).
 - [42] K. Christensen and N. R. Moloney, *Complexity and criticality*, Vol. 1 (World Scientific Publishing Company, 2005).
 - [43] I. Jensen and R. Dickman, *Physical Review E* **48**, 1710 (1993).
 - [44] M. Rossi, R. Pastor-Satorras, and A. Vespignani, *Physical review letters* **85**, 1803 (2000).
 - [45] Y. Ganin, E. Ustinova, H. Ajakan, P. Germain, H. Larochelle, F. Laviolette, M. Marchand, and V. Lempitsky, *The journal of machine learning research* **17**, 2096 (2016).

- [46] D. P. Kingma and J. Ba, Adam: A method for stochastic optimization (2017), arXiv:1412.6980 [cs.LG].
- [47] S. J. Wetzel and M. Scherzer, Physical Review B **96**, 184410 (2017).
- [48] F. D'Angelo and L. Böttcher, Phys. Rev. Research **2**, 023266 (2020).